ISSN 1063-7796, Physics of Particles and Nuclei, 2020, Vol. 51, No. 4, pp. 816–822. © Pleiades Publishing, Ltd., 2020.
Russian Text © The Author(s), 2020, published in Fizika Elementarnykh Chastits i Atomnogo Yadra, 2020, Vol. 51, No. 4.

Resonance Properties of the Josephson Junctions with Ferromagnets

Yu. M. Shukrinov[a, b, *] and I. R. Rahmonov[a, c, **]

[a] *Joint Institute for Nuclear Research, Dubna, 141980 Russia*
[b] *Dubna State University, Dubna, 141980 Russia*
[c] *Umarov Institute of Physics and Technology, Academy of Sciences of the Republic of Tajikistan, Dushanbe, 734063 Tajikistan*
**e-mail: shukrinv@theor.jinr.ru*
***e-mail: rahmonov@theor.jinr.ru*

Received December 20, 2019; revised January 16, 2020; accepted January 29, 2020

Abstract—In the paper, the results of the study of ferromagnetic resonance in a φ_0 junction, in which the phase difference couples directly to the magnetic moment of the barrier, are presented. We have calculated current–voltage characteristics, average superconducting current dependences on the bias current and voltage, and dependences of the maximum amplitude of the magnetization components on the applied voltage at different parameters of spin–orbit coupling. We show the emergence of a constant component of a superconducting current as the effect of coupling between the magnetization and the spin–orbit interaction, and we clarify the role of the coupling in the transformations of current-voltage characteristics occurring in the resonance region. The results presented can be used to develop new resonance techniques for determining the spin–orbit coupling parameter in noncentrosymmetric materials.

DOI: 10.1134/S1063779620040668

INTRODUCTION

Recently, the models describing the interaction of the superconducting current and the magnetic moment in structures of the "superconductor–ferromagnet–superconductor" type, which are important for a number of problems of superconducting spintronics, have been attracting great attention [1–4]. As mentioned in [1], the spintronic research helped to understand fundamental spin-dependent phenomena and to develop applications for new computer technologies. In particular, controlling the magnetic state by superconductivity provides new opportunities for the development of ultrafast cryogenic memory.

The relationship between the Josephson current and magnetization may be due to various causes. Thus, the Rashba-type spin–orbit coupling in a ferromagnet with the broken symmetry of inversion leads to a phase shift in the Josephson junction proportional to the magnetic moment in the barrier. Consequently, the so-called φ_0 junction appears, in which the phase difference couples directly to the magnetic moment of the barrier [5, 6], which determines the unique possibilities to control the barrier magnetic properties by the superconducting current and, in turn, the possibility to influence the Josephson current by the barrier magnetic moment [1–11]. In [3, 6], the authors reported a possibility of reorientation of easy magnetization axis in the presence of spin–orbit coupling. Assuming that the easy axis is initially directed along the z axis, they showed that when the superconducting current was applied, magnetization acquired a certain stable orientation directed between the z and y axes depending on the system parameters. The results obtained provide a possibility to develop an efficient method of determining the values of spin–orbit coupling in ferromagnetic metals.

The Josephson φ_0 junction with the current-phase relation, in which the phase shift is proportional to the magnetic moment perpendicular to the asymmetric spin–orbit potential gradient, displays some unique properties important for superconducting spintronics and modern information technologies. In Ref. [12], we showed that the variation of the current along the current–voltage characteristic (CVC) of the φ_0 junction could lead to both regular and chaotic magnetization dynamics with different specific phase trajectories. Their origin is due to the direct relationship between the magnetic moment and the Josephson current that emerges in these junctions, and the ferromagnetic resonance (FMR), in which the Josephson frequency coincides with the ferromagnetic frequency. It was also shown that the external electromagnetic field could be used to control the magnetic moment dynamics within the current interval corresponding to the Shapiro step, and to make topological transformations of particular precession trajectories. One of the remarkable effects occurring in the φ_0 junction is the emergence of a time independent component of superconducting current [6], which is stipulated by the relation between the magnetization and the spin–orbit coupling.

In Ref. [13], the magnetic moment reversal in the Josephson ϕ_0 junction was studied. Based on the results of the numerical simulation of the magnetic moment component dynamics under the action of a current pulse signal, the full reversal of the magnetic moment was shown at different parameters of the Josephson junction and the signal parameters. The detailed results on the intervals of the dissipation parameter α, ratios between the Josephson energy and the magnetic field energy G, and the spin–orbit coupling parameter r with the full reversal of the magnetic moment were obtained. The periodic reversal was observed intervals with the increase of the ratio between the Josephson energy and the magnetic energy.

In this paper, we investigate the effect of the coupling between the magnetization and the spin–orbit interaction on the phase dynamics, and the features of the ferromagnetic resonance in the φ_0 junction. Based on precision numerical calculations, the manifestation of ferromagnetic resonance is shown in the CVC of the φ_0 junction and in the average superconducting current dependence on the bias current, maximum amplitude $m_y^{\max}$ dependence on the average voltage, and dependences of maximum and minimum values of the amplitude m_y on the bias current. We show that consideration of the Gilbert damping leads to the constant contribution to the Josephson current. This contribution depends on the spin–orbit coupling r and the ratio between the Josephson energy and the magnetic energy G and is absent at $\alpha = 0$. The presence of this constant Josephson current at the constant voltage V applied to the junction means the presence of the dissipative mode, which provides an opportunity for its experimental detection.

1. MODEL

In the Josephson junctions with a thin ferromagnetic layer (F-layer) the superconducting phase difference and magnetization of the F-layer are two related dynamic variables. The system of equations describing the dynamics of these variables follows from the Landau–Lifshitz–Gilbert (LLG) equation and the Josephson relations for the phase difference and the current. In particular, the magnetization dynamics in our system is described by the Landau–Lifshitz–Gilbert equation with the effective field depending on the phase difference

$$\frac{d\mathbf{M}}{dt} = -\gamma\mathbf{M}\times\mathbf{H}_{\text{eff}} + \frac{\alpha}{M_0}\left(\mathbf{M}\times\frac{d\mathbf{M}}{dt}\right),$$
$$\mathbf{H}_{\text{eff}} = \frac{K}{M_0}\left[Gr\sin\left(\varphi - r\frac{M_y}{M_0}\right)\hat{\mathbf{y}} + \frac{M_z}{M_0}\hat{\mathbf{z}}\right], \quad (1)$$

where γ is the gyromagnetic ratio; α is the phenomenological dissipation parameter; φ is the phase difference between the superconductors along the junction; $M_0 = \|\mathbf{M}\|$, $G = E_J/(K\mathcal{V})$, K is the anisotropy constant, $\mathcal{V}$ is the volume of the F layer, $r = lv_{so}/v_F$ is the spin–orbit coupling parameter; v_{so}/v_F characterizes the spin–orbit coupling intensity; v_F is the Fermi velocity; $l = 4hL/\hbar v_F$, L is the length of the F layer; and h denotes the exchange field in the ferromagnetic layer.

Based on the equations for the Josephson junction and magnetic system, we can rewrite the complete system of equations (used in our numerical calculations) in the normalized units:

$$\dot{m}_x = \frac{\omega_F}{1+\alpha^2}\{-m_y m_z + Grm_z\sin(\varphi - rm_y) - \alpha[m_x m_z^2 + Grm_x m_y\sin(\varphi - rm_y)]\},$$
$$\dot{m}_y = \frac{\omega_F}{1+\alpha^2}\{m_x m_z - \alpha[m_y m_z^2 - Gr(m_z^2 + m_x^2)\sin(\varphi - rm_y)]\}, \quad (2)$$
$$\dot{m}_z = \frac{\omega_F}{1+\alpha^2}\{-Grm_x\sin(gj - rm_y) - \alpha[Grm_y m_z\sin(\varphi - rm_y) - m_z(m_x^2 + m_y^2)]\},$$
$$\frac{dV}{dt} = \frac{1}{\beta_c}\left[I - V + r\frac{dm_y}{dt} - \sin(\varphi - rm_y)\right], \quad \frac{d\varphi}{dt} = V,$$

where $\beta_c = 2eI_cCR^2/\hbar$ is the McCumber parameter; $m_i = M_i/M_0$ for $i = x, y, z$; and $\omega_F = \Omega_F/\omega_c$ with the ferromagnetic resonance parameter $\Omega_F = \gamma K/M_0$ and the characteristic frequency $\omega_c = 2eRI_c/\hbar$. Here the time is normalized to ω_c^{-1}, the external current I is normalized to I_c, and the voltage V is normalized to $V_c = I_cR$. This system of equations is solved numerically by the Runge–Kutta method of fourth order, and $m_i(t)$, $V(t)$ and $\varphi(t)$ are determined as the functions of time and external current I. After the averaging procedure [14, 15], the current–voltage characteristic is calculated at the fixed parameters of the system [12]. In order to follow the estimations presented in [6] for the parameter r that is determined by the values of the spin–orbit coupling and the exchange field, we use the values from 0.1 to 1 for r in our calculations.

2. RESULTS OF NUMERICAL CALCULATIONS

Based on the solutions of the system of equations (2), the dynamics of the magnetization component was determined and the CVC of the φ_0 junction was calculated. The calculation parameters are presented in Fig. 1. For each value of the bias current, we determined the maximum and minimum values of the magnetization components, in particular, m_y^{max} and m_y^{min}. In Fig. 1a,

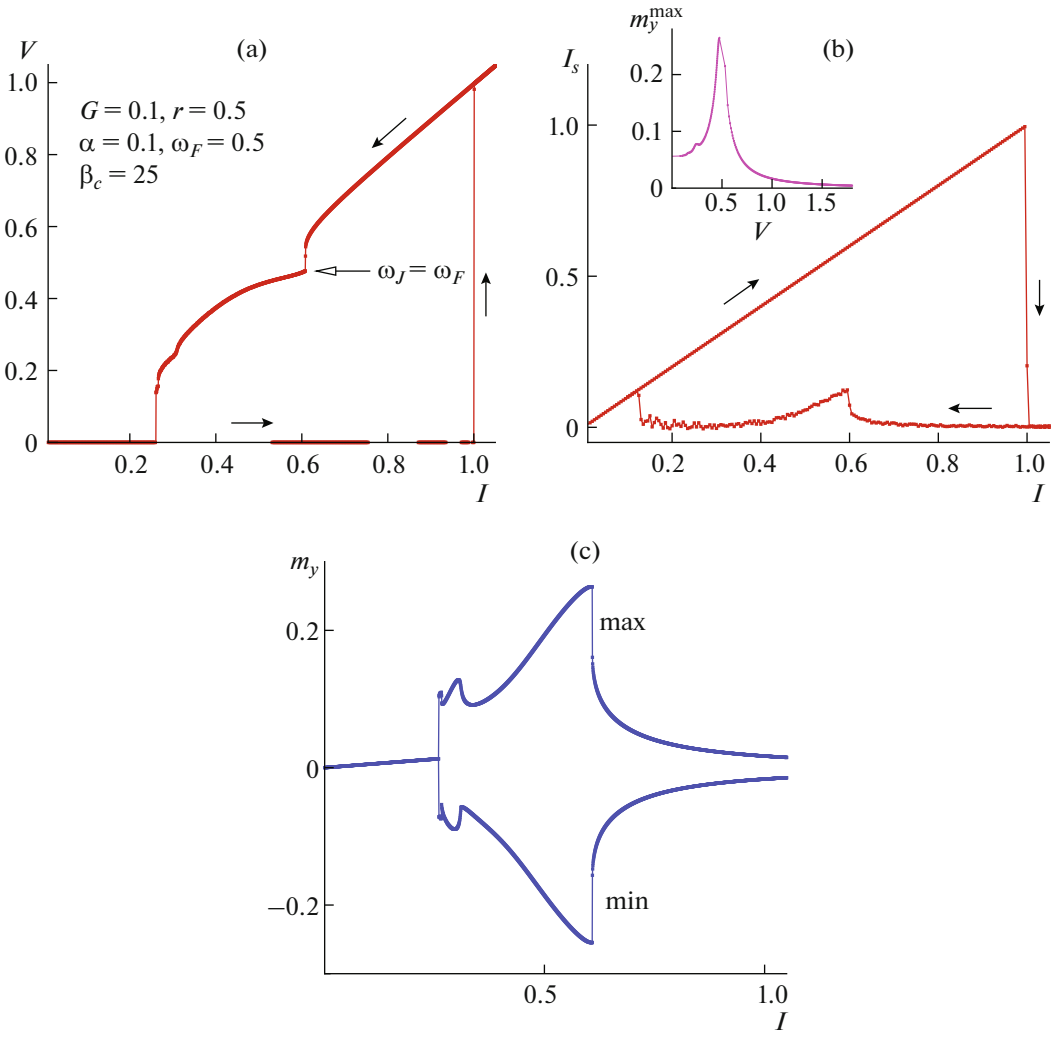

Fig. 1. (a) Manifestation of the ferromagnetic resonance in the CVC of the φ_0 junction and (b) average superconducting current as a function of the bias current. Maximum amplitude $m_y^{\max}$ dependence on the average voltage is shown in the insert; the resonance peak is observed; and (c) dependences of the maximum and minimum values of the m_y amplitude on the bias current.

the CVC of the Josephson φ_0 junction is presented showing the specific behavior near the point where the Josephson frequency coincides with the ferromagnetic frequency, i.e., in the region of ferromagnetic resonance. The dependence of the average value of superconducting current on the value of bias current presented in Fig. 1b also displays a ferromagnetic resonance in the form of maxima at $I = 0.5$. The ferromagnetic resonance is clearly shown in the dependence of the peak value of the oscillation amplitude m_y on the voltage, which is shown in Fig. 1b, inset. The FMR is manifested in the form of growing maximum and minimum amplitudes of oscillations of the magnetization component m_y in the current dependence presented in Fig. 1c. Hence, based on the emerging specific features of the current–voltage characteristic and the current dependence of the maximum and minimum oscillation amplitudes of the magnetization components, which reflect the manifestation of the ferromagnetic resonance, we show the mutual influence of the Josephson current and the magnetization precession in the ferromagnetic layer of the φ_0 junction.

We investigate the effect of spin–orbit coupling on the manifestation of the ferromagnetic resonance in the current–voltage characteristic. In Fig. 2, the parts of current–voltage characteristics of the φ_0 junction are shown for $G = 0.1$, $\alpha = 0.1$, and $\omega_F = 0.5$, at different values of the spin–orbit coupling parameter.

The results presented suggest that a variation of the parameters of the Josephson junction and ferromagnetic layer in a system with damping can lead to a

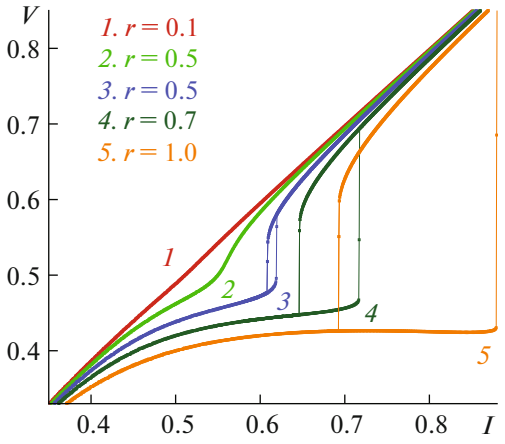

Fig. 2. Manifestation of the ferromagnetic resonance in the current–voltage characteristic. The parts of current–voltage characteristics of the φ_0 junction are shown for $G = 0.1, r = 0.5$, $\alpha = 0.1$, and $\omega_F = 0.5$ at different values of the spin–orbit coupling.

rather strong coupling between the superconducting current and magnetization. This interaction manifested in the CVC of the φ_0 junction near the ferromagnetic resonance is presented in Fig. 2. The direct current contribution to the Josephson current is manifested here as a deviation of the CVC curve from the linear dependence in the resonance region. Note that the observed CVC feature in the resonance region actually reflects the emergence of a resonance branch, which is emphasized by the emergence of the corresponding hysteresis at $r = 0.5$, $r = 0.7$, and $r = 1$. With the increase in the spin–orbit coupling parameter, the rate of growth of the magnetic moment amplitude increases and the length of the resonance branch in the CVC increases, respectively. The mechanism of emergence of this branch is similar to the mechanism observed in the shunted Josephson junctions at the parallel resonance [16, 17], and that of a resonance branch emergence in the CVC of a two-contact SQUID [18, 19].

The corresponding $m_y^{\max}$ dependences on the voltage at different values of the spin–orbit coupling are shown in Fig. 3. The effect of the spin–orbit interaction on the resonance behavior of the presented $m_y^{\max}$ voltage dependence at different values of the spin–orbit coupling parameter can provide a theoretical justification for developing an experimental method for determination of spin–orbit coupling intensity in the noncentrosymmetric materials.

Note that in the equation (the fourth equation in system (2)) of the RCSJ model that describes the φ_0 junction dynamics, the φ phase difference is replaced by $\varphi - r\varphi_0$ to preserve the gauge invariance. The requirement of the gauge invariance leads to an additional term rdm_y/dt in the RCSJ model equation, which was neglected in [12]. In Fig. 3b, the results are presented without considering this term. We see that its contribution does not change the qualitative picture of the phenomenon we described at small values of the spin–orbit coupling parameter r. In both cases, the $m_y^{\max}$ dependences on V almost match each other down to about $r = 0.5$. In Fig. 3c, the results are compared at $r = 0.3$.

3. ANALYTICAL RESULTS AND THEIR COMPARISON WITH NUMERICAL CALCULATIONS

In this section, we compare the results of numerical calculations with the analytical results based on linearization of the LLG equation in the approximation of smallness of parameters of the spin–orbit coupling r and the ratio between the Josephson energy and the magnetic anisotropy energy G. In [6], the dynamics of the system was studied in the approximation of

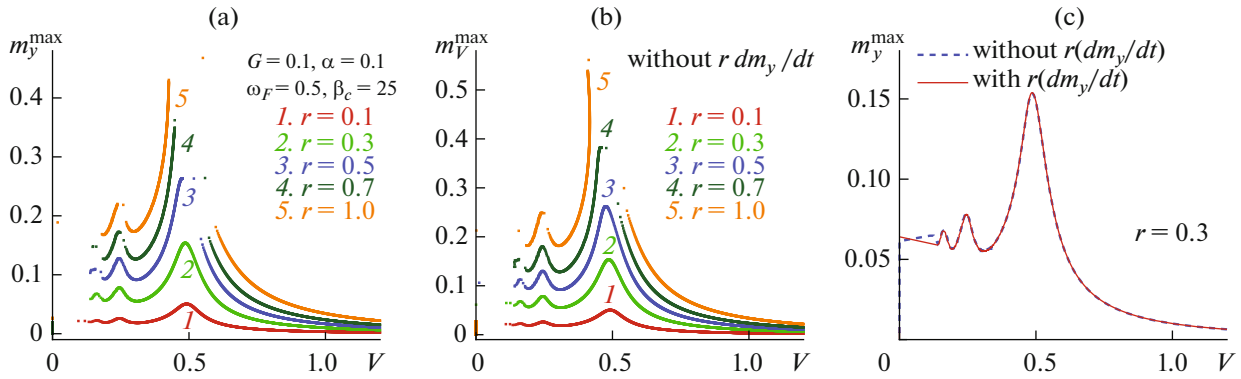

Fig. 3. (a) Maximum amplitude $m_y^{\max}$ dependence on the voltage at different values of the spin–orbit coupling; (b) the same without considering the term rdm_y/dt; and (c) comparison of the results of (a) and (b) at $r = 0.3$.

$\hbar\omega_J \ll T_c$, i.e. when the energy of the Josephson junction and the value of superconducting current are determined by the fixed Josephson frequency ω_J. In this case, the Josephson phase φ can be substituted by $\omega_J t$. This coincides with the point chosen in the CVC of the Josephson junction. In this approximation, the bias current is not considered, which allows comparing the numerical results with the analytical calculations.

First, we consider the magnetic dynamics of system (2) in the case without dissipation ($\alpha = 0$) and the "weak coupling" mode $G \ll 1$, i.e., the Josephson energy E_J is low in comparison with the magnetic field energy E_M. If the voltage is fixed, the last two equations in (2) lead to a linear time dependence of the phase difference $\varphi = Vt$ (Josephson junction with voltage). In our normalization, $V = \omega_J$; therefore, we have $\varphi = \omega_J t$. If other components satisfy the conditions $(m_x, m_y) \ll 1$, then Eqs. (2) can be linearized

$$\begin{cases} \dot{m}_x = \omega_F[-m_y + Gr\sin(\omega_J t)] \\ \dot{m}_y = \omega_F m_x \end{cases} \tag{3}$$

and the corresponding solutions can be written in the following form

$$m_x = \frac{Gr\omega_J\omega_F\cos\omega_J t}{\omega_F^2 - \omega_J^2} \text{ and } m_y = \frac{Gr\omega_F^2\sin\omega_J t}{\omega_F^2 - \omega_J^2}. \tag{4}$$

Thus, the magnetic moment precesses around the z axis. The precessing magnetic moment influences the current in the φ_0 junction

$$\begin{aligned} \frac{I}{I_c} &= \sin(\omega_J t - rm_y) = \sin\left(\omega_J t - r\frac{Gr\omega_F^2\sin\omega t}{\omega_F^2 - \omega_J^2}\right) \\ &= \sin\omega_J t + \frac{Gr^2}{2}\frac{\omega_F^2}{\omega_J^2 - \omega_F^2}\sin 2\omega_J t + ..., \end{aligned} \tag{5}$$

where we have considered that $\dfrac{Gr^2\omega_F^2}{\omega_F^2 - \omega_J^2} \ll 1$. Hence, in addition to the first harmonic oscillations, the current contains higher harmonic contributions. Near the resonance, the harmonic amplitudes increase and change their sign when $\omega_J = \omega_F$. Therefore, the monitoring of the second harmonic of the current oscillations reveals the magnetic system dynamics.

Dissipation plays an important role in the considered system dynamics; when the dissipation is included, this leads to a constant contribution to the Josephson current. Near the resonance $\omega_J \approx \omega_F$, the linearization conditions leading to Eqs. (4) are not satisfied, and the dissipation should be considered. In this case [6], by linearizing the LLG equation in system (2), and accounting for $m_z \approx 1$, and neglecting the quadratic terms m_x and m_y, we obtain:

$$\begin{cases} \dot{m}_x = \dfrac{\omega_F}{1+\alpha^2}\{-m_y + Gr\sin\omega_J t - \alpha m_x\} \\ \dot{m}_y = \dfrac{\omega_F}{1+\alpha^2}\{m_x - \alpha[m_y - Gr\sin\omega_J t]\} \end{cases}. \tag{6}$$

The corresponding expression for m_y in the presence of dissipation can be written as

$$m_y(t) = \frac{\omega_+ - \omega_-}{r}\sin\omega_J t - \frac{\alpha_+ + \alpha_-}{r}\cos\omega_J t, \tag{7}$$

where

$$\omega_\pm = \frac{Gr^2}{2\omega_F}\frac{\omega_J \pm \omega_F}{\Omega_\pm} \text{ and } \alpha_\pm = \frac{Gr^2}{2\omega_F}\frac{\alpha\omega_J}{\Omega_\pm} \tag{8}$$

with $\Omega_\pm = \dfrac{(\omega_J \pm \omega_F)^2 + (\alpha\omega_J)^2}{\omega_F^2}$. Therefore, m_y shows the resonance with dissipation when the Josephson frequency is tuned to the ferromagnetic frequency ($\omega_J \to \omega_F$). In addition, the dissipation leads to the phase oscillations $m_y(t)$ (the term proportional to $\cos\omega_J t$ in Eq. (7)). Finally, the superconducting current

$$\begin{aligned} I(t) = {} & I_c\sin\omega_J t - I_c\frac{\omega_+ - \omega_-}{2}\sin 2\omega_J t \\ & + I_c\frac{\alpha_+ + \alpha_-}{2}\cos 2\omega_J t + I_0(\alpha) \end{aligned} \tag{9}$$

contains the time independent (dc) component

$$I_0(\alpha) = \frac{\alpha Gr^2\omega_J}{4\omega_F}\left(\frac{1}{\Omega_-} + \frac{1}{\Omega_+}\right). \tag{10}$$

The dc contribution shows that the Gilbert damping plays an important role in the φ_0 junction dynamics. This contribution depends on the value of spin–orbit coupling r and the ratio between the Josephson energy and the magnetic energy G; it is absent at $\alpha = 0$.

On the other hand, the presence of the constant Josephson current at the constant voltage V applied to the junction means the presence of a dissipative mode, which can be easily detected experimentally. The emergence of the peak of the direct current near the resonance is similar to the Shapiro step appearance in Josephson junctions in an external electromagnetic field. Note that the presence of the second harmonic in $I(t)$ in Eq. (9) should also lead to half-integer Shapiro steps in the current–voltage characteristics of φ_0 junctions [20].

In Fig. 4a, the maximum amplitude m_y^{max} dependence on the voltage calculated based on system of equations (2), and the analytical dependence $m_y(\omega_J)$ according to formula (7) are presented.

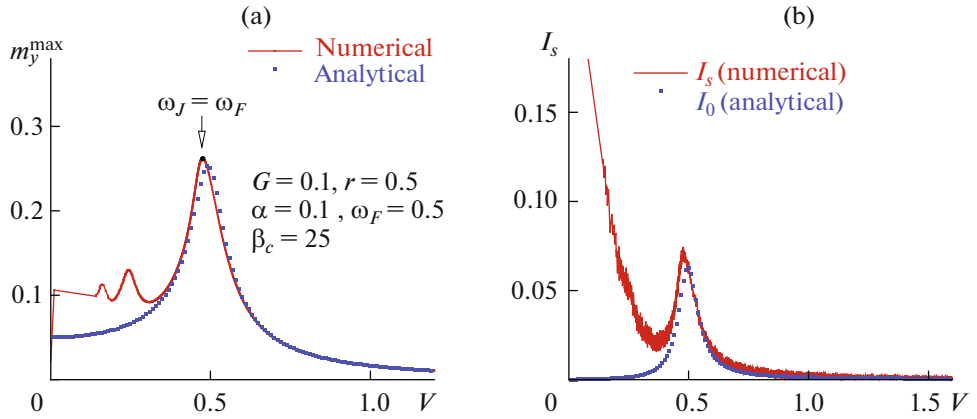

Fig. 4. (a) Maximum amplitude $m_y^{\max}$ dependence on the voltage calculated based on system of equations (2) and analytical dependence $m_y(\omega_J)$ according to formula (7); and (b) superconducting current I_s dependence on the voltage calculated based on system of equations (2), and analytical dependence $I_0(\omega_J)$ according to formula (10).

In Fig. 4b, the superconducting current I_s dependence on the voltage calculated based on the system of equations (2), and the analytical dependence $I_0(\omega_J)$ according to formula (10) are displayed. We can see that the numerical results agree well with the analytical calculations. Note that no approximations are used in the numerical calculations, in contrast to the analytical evaluations (where the weak coupling mode is used and the case of $m_x, m_y \ll 1$ is considered). This is manifested in the special features at $V \approx 0.25$ and $V \approx 0.16$ of the numerically simulated dependence $m_y^{max}(V)$, which reflects the emergence of ferromagnetic resonance harmonics at $\omega_J = \omega_F/2$ and $\omega_J = \omega_F/3$.

4. CONCLUSIONS

We have investigated the features of the ferromagnetic resonance in a φ_0 junction with the direct coupling between the superconducting phase difference and the magnetic moment of the ferromagnetic barrier. Based on precision numerical calculations, the manifestation of ferromagnetic resonance is shown in the CVC of the φ_0 junction and in the average superconducting current dependence on the bias current, maximum amplitude $m_y^{\max}$ dependence on the average voltage, and dependences of maximum and minimum values of the amplitude m_y on the bias current. The Gilbert damping, accounting for which leads to the constant contribution to the Josephson current, plays an important role in the dynamics of the considered system. This contribution depends on the spin–orbit coupling parameter r and the ratio between the Josephson energy and the magnetic energy G; it is absent at $\alpha = 0$. The presence of the constant Josephson current at the constant voltage V applied to the junction means the presence of a dissipative mode, which provides an opportunity for its experimental detection. The presented results on the current–voltage characteristics of the φ_0 junction, the maximum amplitude $m_y^{\max}$ dependence on the average voltage, and the dependences of the maximum and minimum values of the amplitude m_y on the bias current at different spin–orbit coupling parameters might be used to develop new resonance techniques for determining the spin–orbit coupling parameter in noncentrosymmetric materials.

ACKNOWLEDGMENTS

The authors are grateful to A.A. Mazanik for a stimulating discussion of the results presented in this paper.

FUNDING

The study was supported by the Russian Foundation for Basic Research, project nos. 18-02-00318 and 18-52-45011. The numerical calculations were supported by the Russian Science Foundation, project no. 18-71-10095.

REFERENCES

1. A. A. Golubov and M. Yu. Kupriyanov, "Superconductivity: Controlling magnetism," Nat. Mater. **16**, 156–157 (2017).
2. J. Linder and J. W. A. Robinson, "Superconducting spintronics," Nat. Phys. **11**, 307 (2015).
3. Yu. M. Shukrinov, I. R. Rahmonov, K. Sengupta, and A. I. Buzdin, "Magnetization reversal by superconducting current in φ_0 Josephson junctions," Appl. Phys. Lett. **110**, 182407 (2017).
4. L. Cai, D. A. Garanin, and E. M. Chudnovsky, "Reversal of magnetization of a single-domain magnetic

particle by the ac field of time-dependent frequency," Phys. Rev. **B 87**, 024418 (2013).

5. A. I. Buzdin, "Direct coupling between magnetism and superconducting current in the Josephson φ_0-junction," Phys. Rev. Lett. **101**, 107005 (2008).
6. F. Konschelle and A. I. Buzdin, "Magnetic moment manipulation by a Josephson current," Phys. Rev. Lett. **102**, 017001 (2009).
7. I. Žutić, J. Fabian, and S. Das Sarma, "Spintronics: Fundamentals and applications," Rev. Mod. Phys. **76**, 323 (2004).
8. A. A. Golubov, M. Yu. Kupriyanov, and E. Ilichev, "The current-phase relation in Josephson junctions," Rev. Mod. Phys. **76**, 411 (2004).
9. A. I. Buzdin, "Proximity effects in superconductor-ferromagnet heterostructures," Rev. Mod. Phys. **77**, 935 (2005).
10. S. Mai, E. Kandelaki, A. F. Volkov, and K. B. Efetov, "Interaction of Josephson and magnetic oscillations in Josephson tunnel junctions with a ferromagnetic layer," Phys. Rev. **B 84**, 144519 (2011).
11. L. Cai and E. M. Chudnovsky, "Interaction of a nanomagnet with a weak superconducting link," Phys. Rev. B **82**, 104429 (2010).
12. Yu. M. Shukrinov, I. R. Rahmonov, and K. Sengupta, "Ferromagnetic resonance and magnetic precessions in φ_0 junctions," Phys. Rev. **B 99**, 224513 (2019).
13. P. Kh. Atanasova, S. A. Panaiotova, I. R. Rahmonov, Yu. M. Shukrinov, E. V. Zemlyanaya, and M. V. Bashashin, "Periodicity in the appearance of intervals of the reversal of the magnetic moment of a ϕ_0 Josephson junction," JETP Lett. **110**, 722–726 (2019).
14. Yu. M. Shukrinov, F. Mahfouzi, and N. F. Pedersen, "Investigation of the breakpoint region in stacks with a finite number of intrinsic Josephson junctions," Phys. Rev. **B 75**, 104508 (2007).
15. W. Buckel and R. Kleiner, *Superconductivity: Fundamentals and Applications*, 2nd ed. (Wiley-VCH, Wienheim, 2004).
16. Yu. M. Shukrinov, I. R. Rahmonov, and K. V. Kulikov, "Double resonance in the system of coupled Josephson junctions," JETP Lett. **96**, 588–595 (2012).
17. Yu. M. Shukrinov, I. R. Rahmonov, K. V. Kulikov, A. E. Botha, A. Plecenik, P. Seidel, and W. Nawrocki, "Modelling of LC-shunted intrinsic Josephson junctions in high-Tc superconductors," Supercond. Sci. Technol. **30**, 024006 (2017).
18. W.-D. Schmidt, P. Seidel, and S. Heinemann, "On the resonance behaviour of a thin film DC-SQUID," Phys. Status Solidi **A 91**, K155 (1985).
19. I. R. Rahmonov, Yu. M. Shukrinov, and R. Dawood, "Dynamics of a SQUID with topologically nontrivial barriers," JETP Lett. **103**, 395–398 (2016).
20. H. Sellier, C. Baraduc, F. Lefloch, and R. Calemczuk, "Half-integer Shapiro steps at the $0-\pi$ crossover of a ferromagnetic Josephson junction," Phys. Rev. Lett. **92**, 257005 (2004).

Translated by N. Semenova